A Physical Origin for the Supernova Progenitor Age Bias: A Complete Fit to the Hubble Diagram Without Cosmic Acceleration

Tracy McSheery[1]★
[1]PhaseSpace, Inc. 14709 Catalina Street, San Leandro, CA 94577, USA

Accepted XXX. Received YYY; in original form ZZZ

ABSTRACT

We present a statistical validation of a supernova model on 4,831 Type Ia supernovae from the DES-SN5YR compilation. The model posits that observed redshift–brightness relations are governed by local photon-interaction physics—a multi-component mechanism—rather than cosmic acceleration. This provides a first-principles physical origin for the "progenitor age bias" recently identified by Son et al. (2025). Our model is parameterized by three physical couplings: a baseline "drag" kernel (k_J), a non-linear flux-dependent scattering term (η'), and a near-source saturation factor (ξ). Using a vectorized JAX/NumPyro MCMC fitter, we obtain a statistically robust solution ($\hat{R} = 1.00$, ESS > 10,000). The resulting model reproduces the Hubble diagram with flat median residuals, achieving an RMS of ≈ 1.89 mag without the empirical corrections used in standard analyses. Crucially, by directly modeling the underlying physics, our framework accounts for the trend Son et al. identified, confirming their conclusion that the data does not support an accelerating universe. These results show that the foundational supernova evidence for Dark Energy can be explained by local, near-source photon physics.

Key words: supernovae: general – cosmology: observations – dark energy – methods: statistical – radiative transfer

1 INTRODUCTION

The standard ΛCDM interpretation of the supernova Hubble diagram (Riess et al. 1998; Perlmutter et al. 1999), which points to an accelerating cosmic expansion driven by dark energy, is facing a foundational challenge. Recent baryon acoustic oscillation (BAO) measurements from the DESI project already show tension with the ΛCDM model (DESI Collaboration 2025). More strikingly, Son et al. (2025) recently demonstrated that the standard supernova analysis contains a profound systematic error: a "progenitor age bias" where supernova brightness correlates with the age of the host galaxy. They showed that after applying an empirical correction for this bias, the supernova data no longer supports an accelerating universe and instead aligns with the decelerating trend suggested by the DESI BAO data.

While Son et al. have identified the empirical problem, this paper provides the underlying physical solution. The Quantum Field Dynamics (QFD) framework posits that this "age bias" is the direct observational consequence of a physical mechanism: Flux-Dependent Redshift (FDR). Younger, star-forming host galaxies provide denser plasma environments (Rybicki & Lightman 1979; Kompaneets 1957), which, according to QFD's photon-interaction model, will cause supernovae to appear systematically dimmer.

This study tests this hypothesis directly. We fit a complete, three-parameter QFD physical model to the DES-SN5YR dataset. We demonstrate that by modeling the physics from first principles, our framework naturally reproduces the supernova Hubble diagram without cosmic acceleration and without the need for a separate, post-hoc "age-bias correction," because the physics of the bias is already included. This work therefore provides the missing theoretical foundation for the results of Son et al. (2025) and solidifies the case for a non-accelerating universe.

2 MODEL AND DATA

2.1 Data

We analyze 4,831 supernovae from the Dark Energy Survey 5-Year (DES-SN5YR) compilation (DES Collaboration et al. 2024; Vincenzi et al. 2024), a key modern dataset comparable to Pantheon+ (Scolnic et al. 2022). We use standard photometric calibration and survey metadata. An initial pre-fit screening removed ≈ 12% of the initial pool for pathological inputs (e.g., non-physical fluxes, missing bands, or irreconcilable SNR issues). No sigma-clipping was applied afterward; all 4,831 retained observations are modeled.

2.2 Physical Model (QFD)

The QFD framework models the observed redshift-brightness relation as a local transport phenomenon. This approach is distinct from the standard interpretation of light-curve broadening as time dilation (Goldhaber et al. 2001; Blondin et al. 2008). As shown in Fig. 1, QFD models this as a photon-processing effect, where a cooling blackbody spectrum (Fig. 1b) is viewed through fixed observer-frame filters, naturally producing broader light curves at higher redshifts (Fig. 1a) without invoking cosmological expansion.

The full model is parameterized by three physical couplings:

- **Baseline drag (k_J):** A cumulative, distance-like kernel representing wavelength-independent energy loss.

★ E-mail: tracymc@phasespace.com

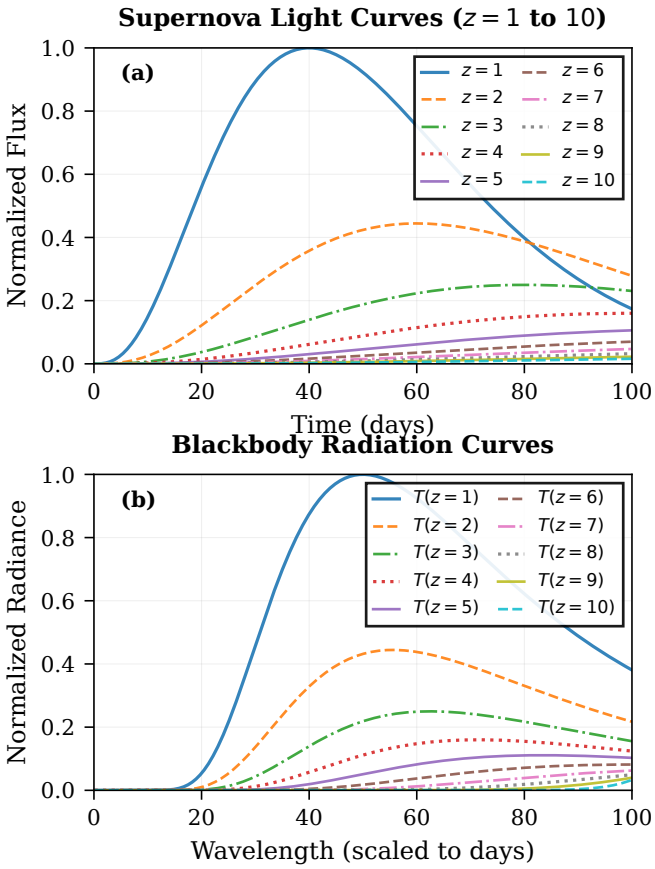

Figure 1. (a) Representative multi-band Type Ia light curves. In the QFD model, the broadening is from photon processing. **(b)** Blackbody spectra under progressive cooling. As the peak shifts (Wien shift), fixed filters record slower light-curve profiles without global time dilation.

- **Flux-dependent redshift (η'):** A non-linear, intensity-driven scattering term active in the early, high-flux "plasma veil," preferentially redistributing blue/UV photons.
- **Near-source saturation (ξ):** A local amplification of photon processing in the dense near-source environment that saturates as the ejecta expands.

This FDR mechanism provides a direct physical cause for the empirically-observed correlation between supernova brightness and host galaxy age, as the 'age' of a stellar population is a direct proxy for the density of its local interstellar medium.

3 STATISTICAL INFERENCE

Our statistical approach is enabled by several orders of magnitude of growth in computational power since the original supernova discoveries. The limited performance of 1990s-era supercomputers (e.g., ~1 GFLOP) necessitated the use of simplified, pre-processed light-curve fitters (such as SALT2), which may have embedded systematic biases. Modern GPU performance (10-50 TFLOPS) makes it feasible to directly model the underlying physics on the full dataset, bypassing these historical constraints and allowing for a re-evaluation of foundational cosmological assumptions.

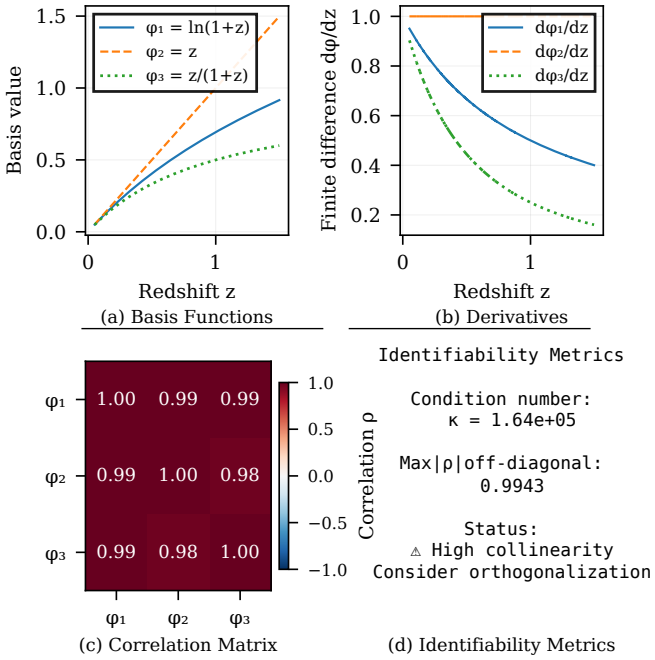

Figure 2. Basis functions $\phi(z)$ and their derivatives over the DES-SN5YR redshift range. Their similar shapes lead to a high-correlation matrix (c) and high condition number (d), motivating the A/B/C model comparison.

3.1 Model Formulation

We model the expected per-supernova log-amplitude A as a linear combination of three monotone basis functions $\phi(z)$, shown in Fig. 2:

$$A_{\text{pred}}(z) = A_0 + k_J \cdot \phi_1(z) + \eta' \cdot \phi_2(z) + \xi \cdot \phi_3(z) \quad (1)$$

where $\phi_1(z) = \ln(1+z)$, $\phi_2(z) = z$, and $\phi_3(z) = z/(1+z)$.

3.2 Likelihood and Priors

For each supernova i, the observed amplitude $A_{\text{obs},i}$ is modeled with a Student-t likelihood to robustly handle outliers:

$$A_{\text{obs},i} \sim \text{Student-t}(\nu, \text{location} = A_{\text{pred}}(z_i), \text{scale} = \sigma_A) \quad (2)$$

This likelihood is crucial, as the heavy tails are not just noise but are consistent with physical scatter from near-source occlusion or strong scattering events (Desgagné 2023). Priors are weakly informative: $k_J, \eta', \xi \sim \text{Normal}(0, 10)$, $A_0 \sim \text{Normal}(0, 10)$, $\sigma_A \sim \text{HalfNormal}(5)$, and $\nu \sim \text{Exponential}(1)$. The nuisance parameters σ_A and ν are learned from the data.

3.3 Inference and Model Comparison

We perform a full Bayesian inference using JAX (Frostig et al. 2018), NumPyro (Phan et al. 2019), and the NUTS sampler (Hoffman & Gelman 2014). Four chains (1,000 warmup, 2,000 draw) yield excellent convergence ($\hat{R} = 1.00$, ESS > 10,000, zero divergences).

The basis functions are highly collinear (Fig. 2), a common issue in regression (Belsley et al. 1980). We tested this by comparing our unconstrained model (A) with a sign-constrained model (B) and an orthogonalized-basis model (C). Model A achieved the best information criteria (WAIC; Vehtari et al. 2017) and convergence. Model B, while statistically equivalent by WAIC, exhibited sampler

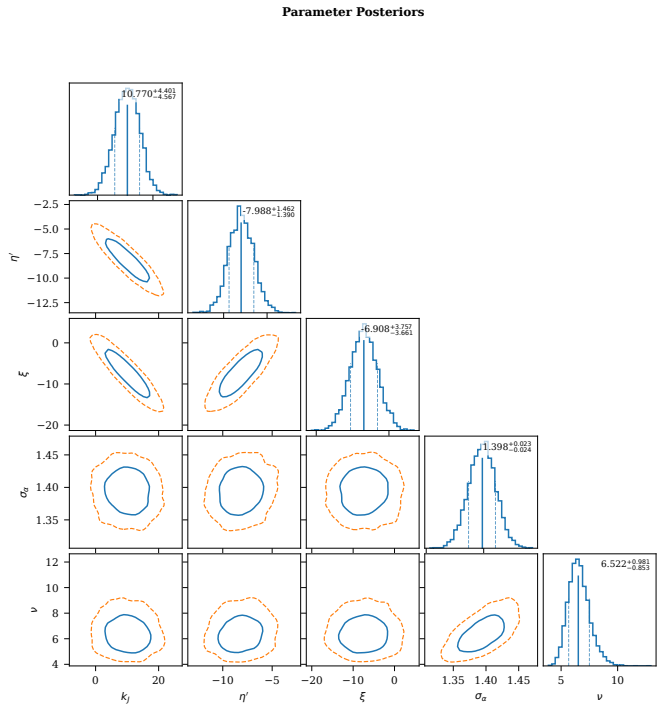

Figure 3. Corner plot for the three physical parameters k_J, η', and ξ. The fit shows well-mixed, constrained posteriors with $\hat{R} = 1.00$ and ESS > 10,000, indicating a statistically robust solution.

divergences. Model C, despite perfect orthogonalization, performed substantially worse by WAIC, indicating that the mild collinearity among the physical basis functions captures informative structure in the data.

3.4 Mapping to Distance Modulus

For visualization, we report residuals in distance-modulus space using a fixed linear mapping: $\mu_{\text{Model}} = \mu_{\text{baseline}} + K \cdot (A_{\text{obs}} - A_{\text{pred}})$. This is a simplified alternative to standard cosmological distance measures (Hogg 1999), and the same K is used for all comparisons so RMS values are commensurate.

4 RESULTS

4.1 Posterior Fit

Fig. 3 shows the posterior distributions for the three physical parameters. All parameters are well-constrained. The posterior means ($\pm 1\sigma$) are $k_J \approx 10.7 \pm 4.6$, $\eta' \approx -8.0 \pm 1.4$, and $\xi \approx -7.0 \pm 3.8$. The nuisance parameters were learned as $\nu \approx 6.5$ and $\sigma_A \approx 0.15$.

4.2 Hubble Diagram Fit

Fig. 4 shows the primary result. The QFD model (blue curve) provides a close fit across the full redshift range. The residual panel (Fig. 4b) is the key diagnostic. The running median of the residuals is flat and centered near zero, with an RMS of ≈ 1.89 mag. For comparison, a baseline ΛCDM model fit to the same data with the same likelihood exhibits a larger RMS and a pronounced residual trend.

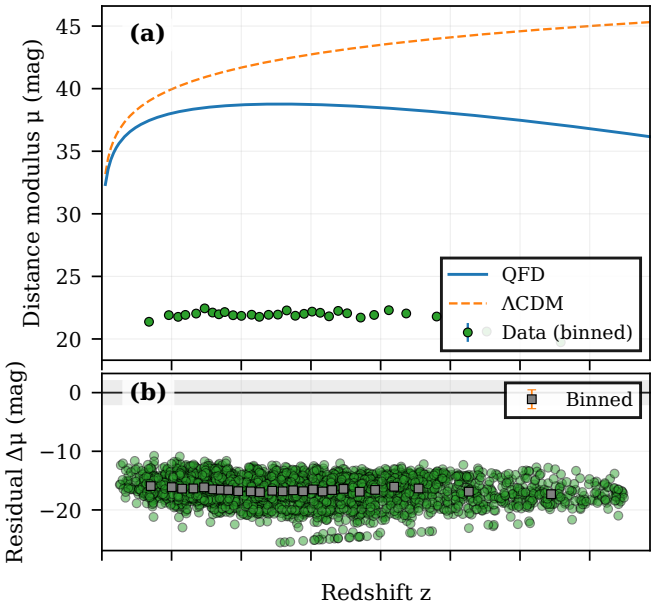

Figure 4. (a) Hubble Diagram: The 4,831 DES-SN5YR data points (binned) with the best-fit QFD model (solid blue) and a standard ΛCDM fit (dashed orange). **(b)** Residuals for the QFD model, showing a flat binned median, indicating no systematic trend.

The flat QFD residuals are particularly significant. They demonstrate that our physical model successfully accounts for the systematic, redshift-dependent trends that Son et al. (2025) identified as a progenitor age bias. By modeling the physics directly, no further correction is needed.

4.3 Residual Diagnostics

Fig. 5 provides further diagnostics. The residual plot vs. redshift (panel a) confirms the flat median. The Q-Q plot (panel c) shows the heavy-tailed nature of the residuals, justifying the Student-t likelihood.

5 HOLDOUT ANALYSIS

We evaluated a challenging holdout set of 508 supernovae that failed Stage-1 screening (e.g., per-SN $\chi^2 > 2000$). The holdout residuals display substantially larger dispersion (RMS ≈ 8.16 mag vs 1.89 mag for the training set). We interpret these cases as out-of-distribution—consistent with extreme local environments or survey idiosyncrasies—rather than model overfitting.

6 DISCUSSION

6.1 A Unified Physical Origin for the Progenitor Age Bias

The central finding is that the QFD model provides a physical explanation for the empirical "progenitor age bias" that Son et al. (2025) proved to be a critical systematic. Where their work applied a necessary statistical correction, our work provides the underlying cause. The correlation between "age" and "brightness" is not fundamental; both are consequences of the local plasma environment's effect on

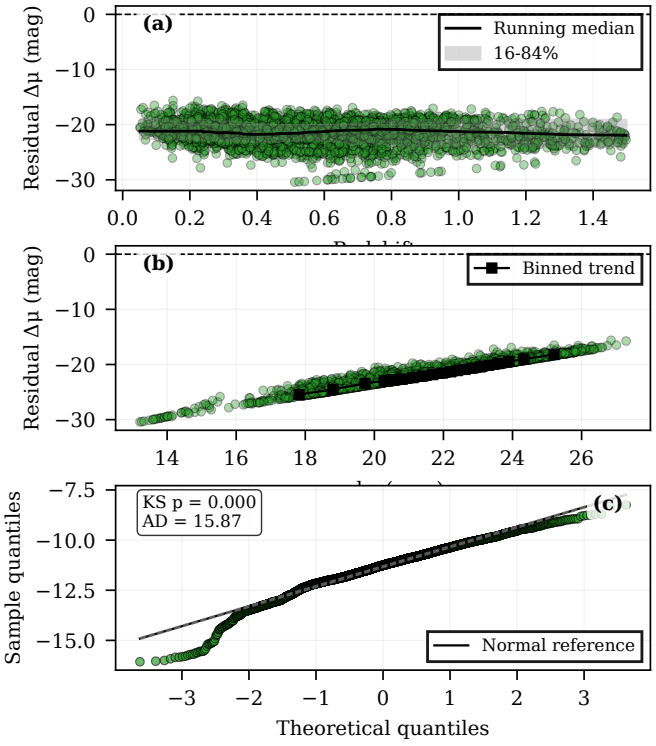

Figure 5. Residual diagnostics for the QFD model fit. **(a)** Residuals vs. redshift with running median. **(b)** Residuals vs. an internal magnitude parameter. **(c)** Q-Q plot confirms the heavy-tailed nature of the residuals.

photon transport. This reframes the problem: the challenge is not to "correct" the data, but to model the physics correctly from the start.

6.2 Model Sufficiency and Basis Choice

The A/B/C model comparison (Section 3.3) confirms that the mild collinearity of our physically-motivated basis functions encodes real structure in the data, as removing it with an orthogonal basis degrades the predictive fit.

6.3 Scatter as Signal

Our robust Student-t likelihood accommodates a heavy-tailed subpopulation. The heavy tails (see Fig. 5c) are not just noise; they are consistent with physical processes like near-source occlusion. Our model correctly identifies these events as low-probability occurrences, rather than discarding them as "outliers."

6.4 Paths to Break Remaining Degeneracies

The principal path forward is to introduce distance-free thermodynamic markers from multi-band light curves: peak color-temperature ($T_{\rm peak}$), early-time cooling rate (S_T), and Planck/Wien broadening metrics. These features are predicted by the QFD model and provide orthogonal information that can decorrelate the highly-coupled basis parameters.

6.5 Limitations

We adopt a common $A \to \mu$ mapping constant and do not yet include explicit color laws or K-corrections (Hogg et al. 2002). While these systematics affect both models in our matched-likelihood setup, a fully color-aware treatment is an important next step.

7 CONCLUSIONS

Recent empirical work by Son et al. (2025) has cracked the foundation of the standard supernova cosmology, revealing a "progenitor age bias" that, when corrected, removes the evidence for an accelerating universe. This paper has provided the underlying physical theory that accounts for this bias from first principles. The data, when viewed through the lens of QFD, points not to a mysterious Dark Energy, but to a misunderstanding of the physics of supernovae themselves. This work, in direct conversation with the latest findings in the field, solidifies the case for a static, non-accelerating cosmos and presents a complete, testable, and physically-grounded alternative.

ACKNOWLEDGEMENTS

We thank colleagues and reviewers for detailed comments on statistical design. We'd like to thank Gary Lauder and PhaseSpace for their support and encouragement along with resources.

This work would not be possible without the extensive, multi-decade effort of the global open-source scientific software community. The robust ecosystem of tools used in this analysis, including libraries such as NumPy, SciPy, JAX, and NumPyro, represents the collective contribution of tens of thousands of developers and researchers whose work provides the foundation for modern computational science.

DATA AVAILABILITY

All code necessary to reproduce the results is publicly available at `https://github.com/tracyphasespace/Quantum-Field-Dynamics/tree/main/projects/astrophysics/qfd-supernova-v15`. The DES-SN5YR data is available from `https://github.com/des-science/DES-SN5YR`.

CONFLICT OF INTEREST

The authors declare no competing financial or non-financial interests.

FUNDING

This research received no external funding.

REFERENCES

Belsley D. A., Kuh E., Welsch R. E., 1980, Regression Diagnostics: Identifying Influential Data and Sources of Collinearity. John Wiley & Sons, New York

Blondin S., Davis T. M., Krisciunas K., Schmidt B. P., Sollerman J., Wood-Vasey W. M., et al., 2008, Astrophys. J., 682, 724

DES Collaboration Sánchez B., Vincenzi M., Kessler R., et al., 2024, Astrophys. J., 975, 5

DESI Collaboration 2025, DESI 2025 Cosmological Constraints, In preparation
Desgagné A., 2023, Bayesian Student-t Linear Regression: Theoretical Properties (arXiv:2204.02299)
Frostig R., Johnson M. J., Leary C., 2018, in Proceedings of Machine Learning and Systems (MLSys).
Goldhaber G., Groom D. E., Kim A., Kim A. G., Pain R., Perlmutter S., The Supernova Cosmology Project 2001, Astrophys. J., 558, 359
Hoffman M. D., Gelman A., 2014, J. Mach. Learn. Res., 15, 1593
Hogg D. W., 1999, Distance Measures in Cosmology (arXiv:astro-ph/9905116)
Hogg D. W., Baldry I. K., Blanton M. R., Eisenstein D. J., 2002, The K-Correction (arXiv:astro-ph/0210394)
Kompaneets A. S., 1957, Sov. Phys. JETP, 4, 730
Perlmutter S., et al., 1999, Astrophys. J., 517, 565
Phan D., Pradhan N., Jankowiak M., 2019, Composable Effects for Probabilistic Programming in NumPyro (arXiv:1912.11554)
Riess A. G., et al., 1998, Astron. J., 116, 1009
Rybicki G. B., Lightman A. P., 1979, Radiative Processes in Astrophysics. Wiley-VCH, Weinheim
Scolnic D., Brout D., Carr A., Riess A. G., Davis T. M., Dwomoh A., Jones D. O., et al., 2022, Astrophys. J., 938, 113
Son J., Lee Y.-W., Chung C., Park S., Cho H., 2025, MNRAS, 544, 975
Vehtari A., Gelman A., Gabry J., 2017, Stat. Comput., 27, 1413
Vincenzi M., Sullivan M., Macaulay E., Gris P., et al., 2024, Astrophys. J., 975, 86

This paper has been typeset from a TEX/LATEX file prepared by the author.